A Novel Compact Broadband Quasi-Twisted Branch Line Coupler Based on Double-Layered Microstrip Line

Fayyadh A. H Ahmed * , Rola Saad , Salam K Khamas

Posted Date: 18 December 2023

doi: 10.20944/preprints202312.1281.v1

Keywords: Branch Line Coupler (BLC); microstrip double-layered TL (MDL-TL); phased array antenna; slow wave structure

Article

A Novel Compact Broadband Quasi-Twisted Branch Line Coupler Based on Double-Layered Microstrip Line

Fayyadh A. Ahmed *, Rola Saad and Salam K. Khamas

Communications Research Group, Department of Electronic and Electrical Engineering, University of Sheffield, Sheffield S1 3JD, UK;

* Correspondence: fhahmed1@sheffield.ac.uk

Abstract: A novel quasi-twisted miniaturized wideband Branch Line Coupler (BLC) is proposed. The design is based on bisecting the conventional microstrip line BLC transversely and folding bisected sections on double-layered substrates with a common ground plane in between. The pair of quarter wavelength horizontal parallel arms is converted to a Z-shape meandered microstrip line in the designed structure. On the other hand, the pair of quarter wavelength vertical arms are cut by half into two lines and converted to a periodically loaded slow wave structure. The bisected parts of BLC are placed on the opposite side of the doubled-layer substrate and connected through four vias passing through the common ground plane. This technique enabled a compact BLC size of 6.4×18 mm^2, which corresponds to a surface area miniaturization by ~50% as compared to the classical BLC size of 10×23 mm^2 at 6GHz, Moreover, the attained relative bandwidth is 73.9% (4.6-10 GHz) for S_{11}, and 75.8% (4.5-10 GHz) for S_{33} as compared to 41% for the ordinary BLC at the same resonant frequency. The circuit is constructed on a double-layered low-cost FR4 substrate with a relative permittivity of 4.3, and a loss tangent of 0.025. An isolation of -13dB was realized in both S_{13} and S_{31} demonstrating an excellent performance. The transmission coefficients between input/output ports S_{21}, S_{41}, S_{23}, and S_{43} are between -3.1dB to -3.5dB at the frequency of 6GHz. Finally, the proposed BLC provides phase differences between output ports of 90.5^o and 94.8^o at the frequency of 6GHz when the input ports 1 and 3 are excited, respectively. The presented design offers the potential of being utilized as a unit cell for building a Butler-matrix (BM) for sub-6GHz 5G beamforming networks.

Keywords: Branch Line Coupler (BLC); microstrip double-layered TL (MDL-TL); phased array antenna; slow wave structure

1. Introduction

Beam scanning antennas play a key role in 5G communication system to attain the desired output. The use of beamforming feeding networks (BFNs) is an essential technique to obtain high directivity in a particular direction and improve the connection quality as well as coverage for the 5G system [1]. The function of BFNs is to adjust the phase and amplitude of feeding signals for phased array antenna systems [2]. Butler-matrix (BM) is one of the most common BFNs of 5G systems owing to distinctive features such as simplicity, lower-cost, and easy fabrication process. In addition, BM doesn't need external biasing in its operation. Besides, BM operates as a reciprocal feeding system for transmitting and receiving signals in phased array antenna systems. The building block of the BM is the BLC, which can be utilized as a modulator, mixer, and phase shifter, as well as its basic function as part of a feeding network of phased array antenna system [1]. Therefore, this work focuses on the design of a compact BLC with enhanced bandwidth. As illustrated in Figure 1, a BLC consists of four transmission lines grouped into two pairs, with each pair consisting of parallel horizontal and vertical lines. The characteristics impedance of the horizontal lines is $Z_o/\sqrt{2}$ while for the vertical counterparts it is Z_o, where Z_o represents the characteristics impedance of the microstrip transmission line (MSTL). Each of the four transmission lines (TL) has a length of $\lambda_g/4$, where λ_g is the guided wavelength. Thereby the dimensions of the BLC are primarily based on the operating

frequency, thus in low-frequency the BLC extend over a large area of the host device board, and hence lead to an increased size [3]. Another inherent issue with a conventional BLC is the limited bandwidth characteristics of no more than 50%, which restrict their applications and would require a large multi-sections circuit to gain wideband characteristics, which in turn increases the circuit's area [4].

Many efforts have been reported that address the above limitations. For example, the coupled line unit cells concept was introduced in [3] to create a dual composite Right/Left-handed (D-CR/LH) unit cell, which results in a design that has a miniaturized area of ~ 52% of that of a conventional BLC at 1.8GHz with a relative bandwidth of 18 %. T-shaped slots and open stubs were employed in the horizontal and vertical arms of the BLC, resulting in a 30% bandwidth improvement and a 12.3% size reduction [4].

In another study, a double-layer board with slow-wave microstrip transmission lines and blind vias was used to achieve a 43% size reduction compared to a conventional design at the same resonant frequency. However, the increased number of vias led to higher insertion losses and design complexity [5]. A Koch fractal-shape BLC of various iterations was suggested in [6], where the sample was designed to operate at 2.4GHz and offered a size reduction of ~81% in combination of a relative bandwidth of 33%.

In [7], open-ended stubs and transmission line meandering with a stepped impedance approach have been proposed with a size reduction of ~61% and 50% compared to a conventional BLC, respectively. However, the narrow bandwidth of ~130 MHz represents a key limitation. A flexible coupler using a Teslin paper substrate was reported [8]. It replaced the conventional quarter-wavelength transmission lines with a collective of shunt open-stubs, series transmission lines, and meandered lines, resulting in a compact design with a surface area of 0.04 λ_g^2, and a 68% fractional bandwidth. Using a dual microstrip transmission line, the BLC size was reduced by 32% with a fractional bandwidth of 60% [9]. However, this approach had poor return losses over the operating bandwidth. To improve matching, T-shaped transmission lines were used, reducing fractional bandwidth and size to 50% and 44%, respectively. A compact BLC class introduced a prototype using open-circuited stubs to replace traditional quarter-wavelength transmission lines [10], resulting in a ~55.6% size reduction and achieving 11% and 50% fractional bandwidth for narrowband and wideband modes of operation, respectively.

In [11], a new configuration, BLC, is presented. The design applies two types of trapezoid-shaped resonators on the arms of the BLC to configure a wideband branch-line coupler. The proposed design has achieved a size reduction of 79% compared to conventional couplers. In addition, it offered a fractional bandwidth of 22.2%. [12] used artificial transmission lines (ATL) for miniaturization. They replaced conventional transmission lines with right-handed transmission lines (RHTL) and constructed the branch-line coupler sides using cascaded T-Net RHTLs instead of quarter-wavelength transmission lines. This design achieved a 50% size reduction compared to the conventional BLC and a 33.3% fractional bandwidth (2.0–2.8 GHz). A simple method was used to improve bandwidth in [13]. By adding a single transmission line element to a conventional coupler, they increased bandwidth by approximately 25%. However, the proposed structure is larger at 25.7×22.8mm compared to the conventional coupler's 21.5×20.7mm.

Triangular and trapezoidal resonators were added to the coupler for miniaturization and harmonic suppression [14]. The design achieved an 84% size reduction and wide harmonic suppression. However, it has a complex structure with a low-frequency band around 200MHz, representing a 26% fractional bandwidth (FBW).

The majority of the aforementioned prototypes were based on composite Right/Left-handed structures to create the branch lines, which might result in unfavorable characteristics that are associated with miniaturization such as shallow return losses for input ports, poorly isolated ports, and narrow bandwidth in some cases [3,4,6,8]. In addition, the structures of Right/Left-handed transmission line probably increase the structure's complexity, which results in a challenging practical realization despite the overall size reduction.

In this study, a quasi-twisted shape branch line coupler is proposed, which is the longitudinal bisection of the conventional BLC into two sections and twisting each over the other. The structure is

Preprints (www.preprints.org) | NOT PEER-REVIEWED | Posted: 18 December 2023 doi:10.20944/preprints202312.1281.v1

designed based on the microstrip double-layered TL (MDL-TL). The input/output transmission lines and horizontal arms of the BLC are built based on Z-shape meandered section with round blend edges, while $\lambda_g/4$ vertical arms of BLC are adopted for the slow wave structure. The MDL-TLs are placed on two layers and were connected using four conductive vias. A common ground plane is placed between the layers of the MDL-TLs, which incorporates circular slots around the vias to avoid shorting them to the common ground plane. The described configuration reduced the size of the conventional BLC by 49.9 % and improved the relative bandwidth to 75.8%. The novel design is modelled and simulated using Computer Simulation Technology (CST) microwave studio and then fabricated and tested on a low-cost FR-4 substrate material demonstrating promising S-parameter results.

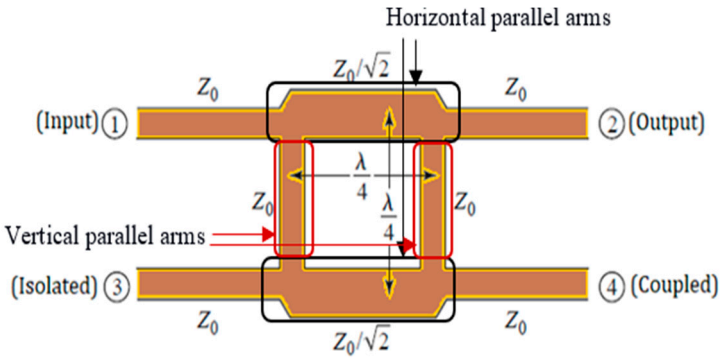

Figure 1. Geometry of a branch-line coupler.

The paper is organized as follows: Section 2 explains the theoretical analysis and design procedures of developing a wideband MDL-TL and comparing the achieved performance with that of a conventional microstrip line; Section 3 presents the analysis and design of a branch line coupler based on MDL-TL. Finally, Section 4 presents the simulated and measured results demonstrating the novel BLC performance.

2. Theory

2.1. Selection of the Classical Microstrip Line Dimensions

The Microstrip Transmission Line (MSTL) represents the building block of any passive and active microwave device due to a number of advantages such as the easy fabrication process as well as the availability of numerous miniaturization approaches [15]. Microstrip line connector of width W is placed on a grounded thin dielectric substrate of height h and dielectric constant of ε_r. For a particular characteristic impedance, Z_0, the ratio of the line width (W) to the substrate height (h) is given by [15]:

$$\frac{W}{h} = \begin{cases} \dfrac{8e^A}{e^{2A}-2} & for\ W/h < 2 \\ \dfrac{2}{\pi}\left[B-1-\ln(2B-1)+\dfrac{\varepsilon_r-1}{2\varepsilon_r}\left\{\ln(B-1)+0.39-\dfrac{0.61}{\varepsilon_r}\right\}\right] & for\ W/h > 2 \end{cases} \quad (1)$$

where

$$A = \frac{Z_o}{60}\sqrt{\frac{\varepsilon_r+1}{2}} + \frac{\varepsilon_r-1}{\varepsilon_r+1}\left(0.23+\frac{0.11}{\varepsilon_r}\right), \text{ and } \qquad B = \frac{377\pi}{2Z_o\sqrt{\varepsilon_r}}$$

The microstrip physical length l that is required to generate a phase shift (delay) of θ can be determined as:

$$\theta = \beta l = \sqrt{\varepsilon_e}\, k_o l \quad (2)$$

Preprints (www.preprints.org) | NOT PEER-REVIEWED | Posted: 18 December 2023 doi:10.20944/preprints202312.1281.v1

where f and c are the frequency and speed of light, respectively, $k_o = \frac{2\pi f}{c}$, ε_e is the effective dielectric constant, which is in the range of $1 < \varepsilon_e < \varepsilon_r$

2.2. The Impact of Right-Angled Bend on the Performance of the Microstrip line

Complex microwave circuits usually comprise bend microstrip transmission lines, and quite often the width of the line does not change across the bend. Figure 2 illustrates a right-angled bend MSTL with its equivalent circuit. The bend MSTL generates a capacitance C_{bend} and inductance L_{bend}, which result in gathering additional charge at the line corner in particular at the outer edge of the bend area, whereas the inductance arises due to disruption of the current flow [16]. The closed formulas of the bend's capacitance and inductance are [16]:

$$\begin{cases} \dfrac{C_{bend}}{W} = \dfrac{(14\varepsilon_r + 12.5)\,W/h - (1.83\varepsilon_r - 2.25)}{\sqrt{W/h}}\ \dfrac{\text{pF}}{\text{m}}, & W/h < 1 \\ \dfrac{C_{bend}}{W} = (9.5\varepsilon_r + 1.25)\dfrac{W}{h} + 5.2\varepsilon_r + 7.0\ \dfrac{\text{pF}}{\text{m}}, & W/h > 1 \end{cases} \quad (3)$$

and

$$\frac{L_{bend}}{h} = 100\left[4\sqrt{\frac{W}{h} - 4.21}\right]\ \text{nH/m} \quad (4)$$

When $0.5 \leq \frac{W}{h} \leq 2$

Generally, performance and bandwidth enhancement of the microstrip line-based circuit is realized by compensating bend discontinuities. This is usually implemented by chamfering or rounding the corners, which leads to minimizing the reactance. The percentage chamfer M is given by $(x/d)\times 100\%$, where x/d is chamfered to bend diagonal ratio at the bending corner as in Figure 2c and can be determined using [16]:

$$M = 52 + 65e^{(-1.35W/h)} \quad (5)$$

which is valid for $W/h \geq 0.25$ and $\varepsilon_r \leq 25$.

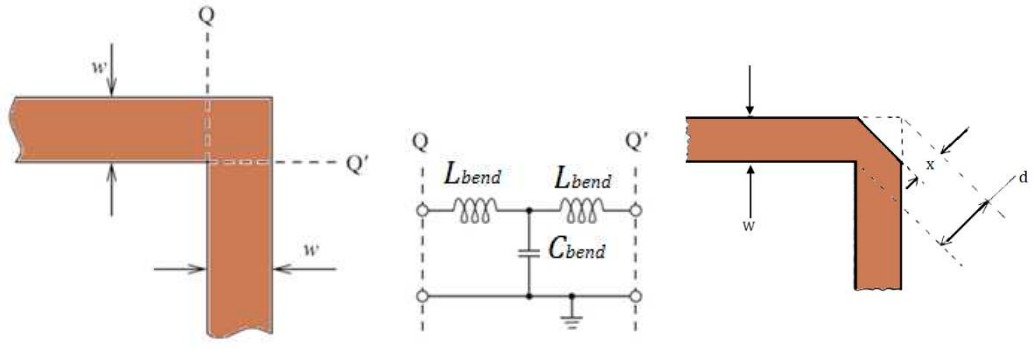

(a) (b) (c)

Figure 2. (a) Part of bend microstrip line, (b) Equivalent circuit, (c) Chamfered right-angled bend microstrip line.

In this work, the MDL-TL is used as a unit cell to build the BLC this line is bent over a horizontal, *xy*-plane and vertical, xz or yz, planes when folded around double-layer substrates. The normal even- and odd-mode theory can be used to analyze the port parameters of a pair of quasi-twisted MDL-TL.

The schematics of the meandered Z-shaped MSTL in even and odd modes are demonstrated in Figure 3a,b. The C_{mx} and C_{my} are the coupling capacitance in the x and y directions, respectively, factor 2 arise due to double-layered structure around the common ground plane, and C_{my} is much stronger than C_{mx}. Therefore, it can be neglected [17]. The difference of characteristic impedance between the

Preprints (www.preprints.org) | NOT PEER-REVIEWED | Posted: 18 December 2023 doi:10.20944/preprints202312.1281.v1

even and odd modes can be negligible since the coupling between top and bottom MSTL is very small and they are given as in[17]:

$$Z_{0e} = Z_0\sqrt{\frac{1+C}{1-C}} \quad , Z_{0o} = Z_0\sqrt{\frac{1-C}{1+C}} \tag{6}$$

where C is the coupling factor.

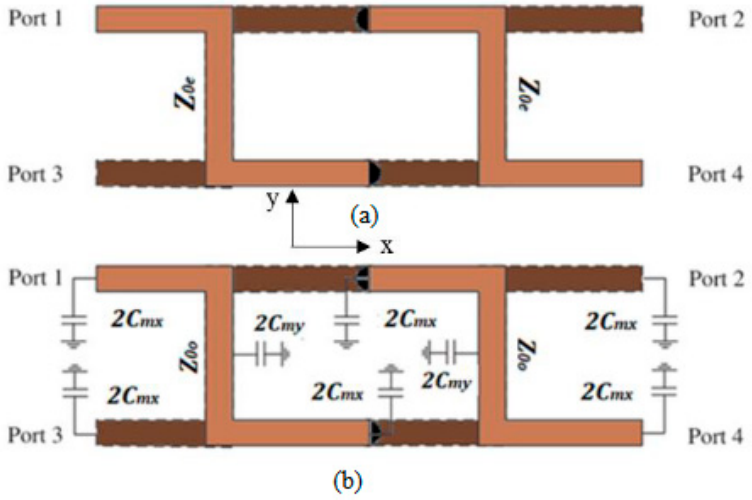

Figure 3. Double layered MSTL equivalent model (a) Even mode. (b) Odd mode.

2.3. Study the Effect of two-dimensional Meandering on the Performance of the Proposed MDL-TL.

This section aims to assess the effectiveness of the MDL-TL structure compared to a conventional microstrip transmission line by examining its S-parameters and compared them with the conventional ones. In order to create an MDL-TL structure from a conventional MSTL, four stages of modification are being undertaken, and can be observed in Figure 4. These stages included the one-layered conventional MSTL, the one-layered meandered MSTL without and with chamfering, and the double-layered with chamfering (MDL-TL). The effect of meandering of the structure varying the line length over xy-plane and x-z plane was conducted on an FR-4 substrate with a dielectric permittivity of 4.4 and a loss tangent of 0.025, and a substrate thickness of 0.8 mm at 6 GHz. This investigation includes a comparison of the key parameters of the four-line configurations, namely the reflection coefficient (S_{11}), transmission coefficient (S_{21}) and phase of S_{21} (or output phase).

In this study, a specific section of a $\lambda_g/2$ length transmission line at 6 GHz, which corresponds to a physical length of 13.8mm, was chosen. The width of the line has been set at 1.52 mm to maintain a characteristic impedance of 50Ω. The transmission line was transformed into a meandered Z-shape and then into an MDL-TL configuration using vias with diameters equal to the width of the microstrip line. The meandered Z-shape has a length of 8.76mm, while the MDL-TL configuration has a length of 5.18mm, as illustrated in Figure 4.

Preprints (www.preprints.org) | NOT PEER-REVIEWED | Posted: 18 December 2023 doi:10.20944/preprints202312.1281.v1

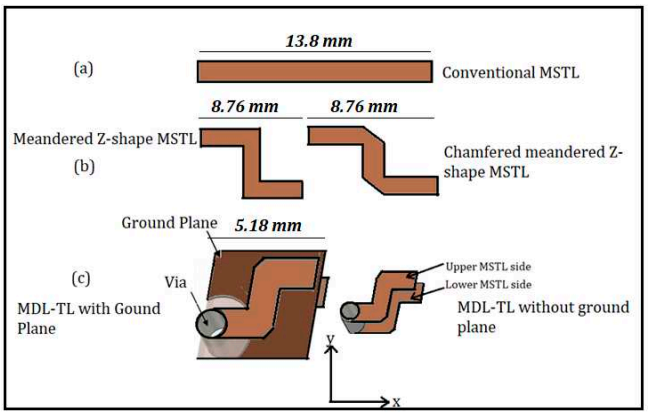

Figure 4. Various MSTL configurations; (a) Single layer straight MSTL, (b) Single layer meandered MSTL, (c) Double layer meandered MSTL.

Figure 5a demonstrates the reflection coefficient, S_{11}, of the four types of lines, where it can be noted how meandering the line without applying chamfering technique deteriorates the impedance matching at the input ports by increasing S_{11} from -30dB to -18dB at the target frequency of 6 GHz. This attributed to the emergence or occurrence of bending parameters like $C_{\_bend}$ and $L_{\_bend}$, as explained earlier in the equations (3) and 4. However, it is clear from Figure 5a also how chamfering the corners provided discontinuity substitution and improved the matching again by reducing S_{11} to ~ -38dB. It can also be noticed that the S_{11} of the MDL-TL are as well matched as the conventional MSTL, at 6GHz. Moreover, the proposed MDL-TL structure offers as good matching as conventional line as it has almost equal and lower S_{11} than conventional line especially at the target frequency of around 6GHz.

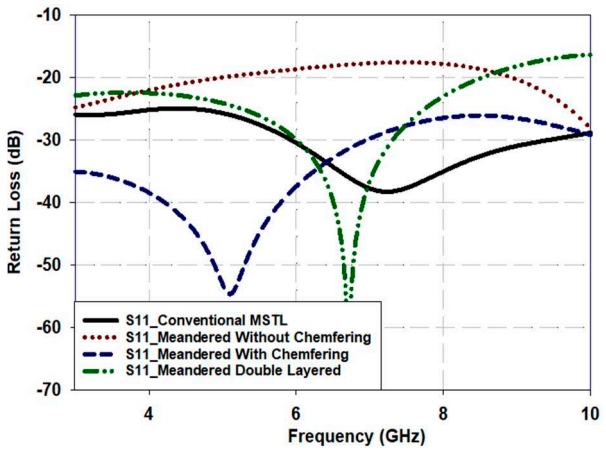

(a)

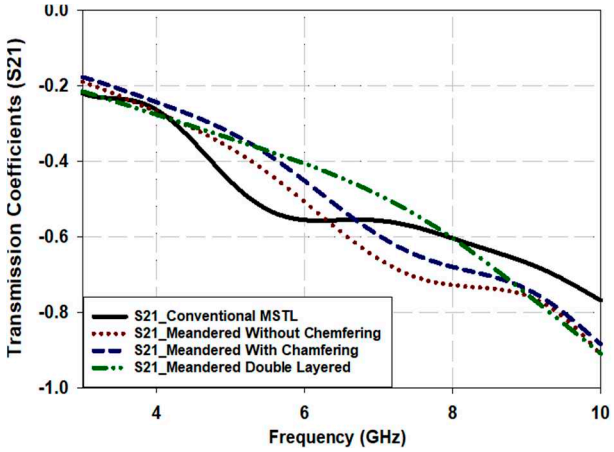

(b)

Preprints (www.preprints.org) | NOT PEER-REVIEWED | Posted: 18 December 2023 doi:10.20944/preprints202312.1281.v1

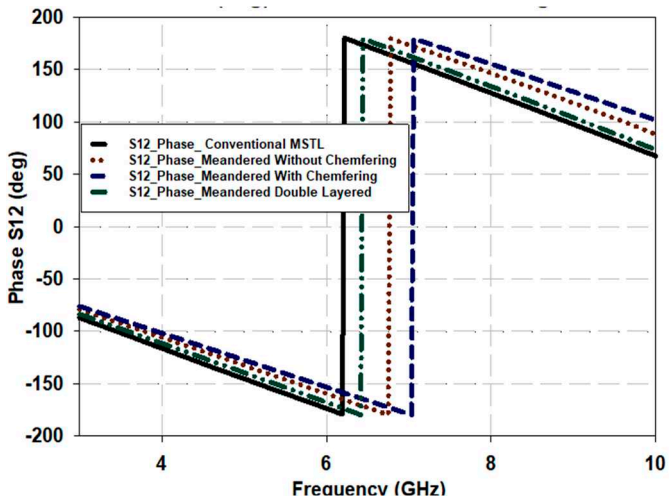

(c)

Figure 5. Performance of different MSTL configurations; (a) $|S_{11}|$, (b) $|S_{21}|$, (c) Phase of S_{21} (Output phase).

Figure 5b, demonstrates the transmission coefficients of all line configurations, where it can be noted that adjusting MSTL with meander, chamfering etc. of one-layered MSTL does not have much effect on the transmission coefficient since S_{21} within -0.45dB to -0.55dB at 6 GHz. Furthermore, S_{21} of the double layered MSTL is higher by about 0.075 dB in the frequency range of 6GHz to 7GHz, this confirms good performance compared to a conventional MSTL. On the other hand, the output phases of all configurations have approximately the same phase delay of 180° since the MSTL is modeled with an electrical length of $\lambda_g/2$ at 6 GHz as presented in Figure 5c. It should be noted that the same results have been obtained when port 2 is considered as the input port and they have been omitted for brevity. The achieved results confirm that the proposed configuration can be utilized as a unit cell for compact-size structures with improved performance.

3. Branch Linee Coupler's Design

3.1. Conventional Branch Line Coupler

Figure 6 shows a 10 mm × 23 mm conventional BLC designed at 6GHz on an FR4 substrate with a thickness of 0.8 mm and dielectric constant (ε_r) of 4.4 with a loss tangent of 0.025, the same substrate specification as the proposed BLC for effective comparison. The 50 Ω microstrip line sections for ports 1,2,3, and 4 are designed with a width of 1.52 mm and the $\lambda_g/4$ sections of the coupler, of impedance $Z_0/\sqrt{2}$ (35.35 Ω) are of a microstrip line with a width of 2.62 mm, as shown in Figure 6.

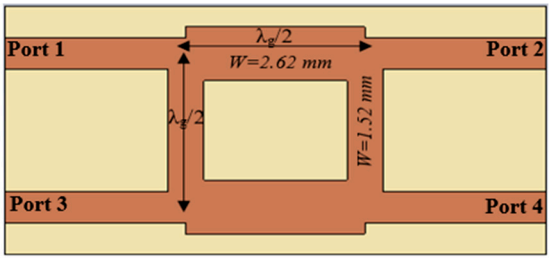

Figure 6. Structure of the conventional branch coupler operating at 6 GHz.

Figure 7 shows the simulated scattering parameters for the conventional branch line coupler, operating at 6GHz. The input reflection coefficient (S_{11}) and the isolation coefficient between input ports S_{31} are presented in Figure 7a, demonstrating a -30dB excellent match for the conventional BLC at the frequency of interest, 6 GHz, alongside a relative impedance bandwidth of 42.2% (5.214 GHz – 8 GHz), in addition to a perfect isolation of -50 dB. On the other hand, Figure 7b illustrates the

Preprints (www.preprints.org) | NOT PEER-REVIEWED | Posted: 18 December 2023 doi:10.20944/preprints202312.1281.v1

transmission coefficient (S_{21}) and coupling coefficient (S_{41}), where it can be shown that the power is divided equally between the output ports (2 and 4) at 6.18 GHz, with a value of -3.8 dB. However, the delivered power declines in both output ports (2, and 4) as the frequency increases, reaching -5.6 dB at the transmission port (port 2) and -6.38 dB at the coupled port (port 4), as shown in Figure 7b.

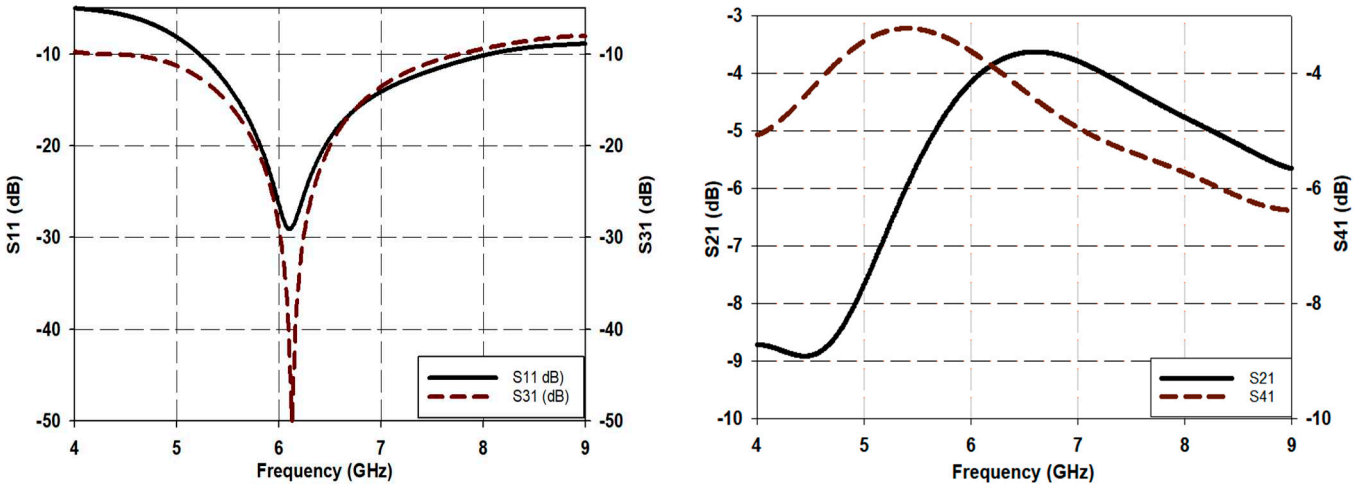

Figure 7. Scattering parameters of conventional BLC; (a) reflection coefficient (S_{11}) and isolation coefficient (S_{31}), (b) Transmission coefficient (S_{21}) and coupling coefficient (S_{41}).

3.2. Proposed Quasi-Twisted Branch Line Coupler Structure

A branch line coupler incorporating a MDL-TL topology has been designed on a double layered 0.8-mm FR-4 substrate, as shown in Figure 8. The horizontal $\lambda_g/4$ dimensions of the conventional branch line coupler of Figure 1 have been transformed to an MDL-TL-based Z-shape, while the vertical $\lambda_g/4$ dimensions have been converted to a periodically loaded open-stub configuration (slow wave structure) to achieve a compactness in the structure. Figure 8a presents a perspective view of the proposed design. The preliminary dimensions of the suggested BLC were selected based on equations (1) and (2) for the conventional MSTL's width and length, respectively. These dimensions were then slightly optimized using CST. The bending of the meandered Z-shape of the MDL-TL generates a certain reactive component that negatively affects the transmission line performance, such as reflection and transmission coefficients. Therefore, to compensate for this reactance, a 1.5mm radius round-chamfered was implemented at the bending of the MDL-TL. A summary of the designed BLC specifications is presented in Table 1. The proposed branch line coupler configuration has a quasi-twisted structure as illustrated in the view of Figure 8b.

Preprints (www.preprints.org) | NOT PEER-REVIEWED | Posted: 18 December 2023 doi:10.20944/preprints202312.1281.v1

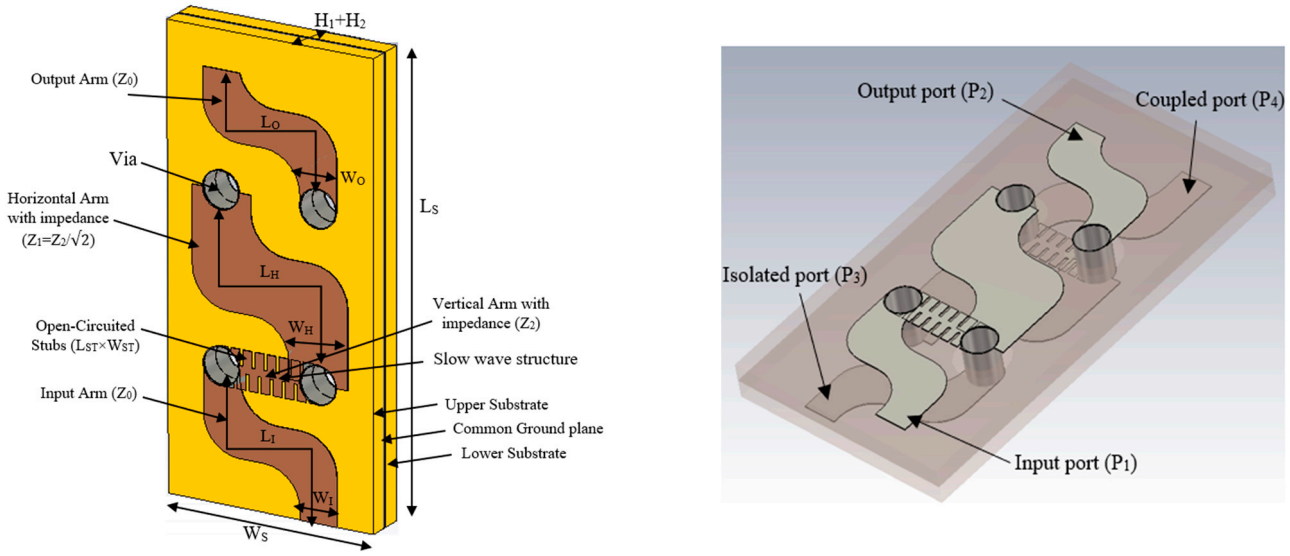

Figure 8. Proposed quasi-twisted branch line coupler; (a) Perspective view, (b) frame mode view.

The proposed design concept is inspired by twisted cable shapes, aiming to substantially reduce the blank space occupied by traditional BLC circuitry. This was accomplished by dividing the conventional BLC horizontally and interweaving the upper and lower segments in a twisted fashion, utilizing a Z-shaped meandering technique with traditional MSTL components. The design procedure of the suggested BLC of Figure 8 involves two key steps as follows:

Step1: As shown in Figure 8, the characteristic impedance of the input, output, coupled, and isolated ports has been selected to be Z_0=50Ω. Also, using equation (1) the relevant lines' $\lambda_g/4$ MSTL (the four input/output ports), shown in Figure 8, are designed of a width is 1.53mm. On the other hand, the width of the horizontal characteristic's impedance of $Z_1= Z_0/\sqrt{2}$, has been calculated as 2.63mm, and further optimized to 2.42mm to realized optimal s-parameters performance. The vertical $\lambda_g/4$ length arms with an impedance of $Z_2=Z_0$ are designed to occupy an optimal small area. The internal and external corners of all the Z-shaped sections are round-chamfered having a radius of 1.5mm to improve the reflection and transmission coefficients as described in Section 2. The length, L_o, of the output port (P_2) is less than $\lambda_g/4$, which in turn is shorter than the L_c length of the coupled port (P_4), as shown in Figure 8b. These modifications in the lengths are necessary to tune the difference between the output ports' phases to ~90°. The proposed structure, demonstrated in Figure 8, provides a novel BLC configuration, which is significantly miniaturized by ~50% as compared to a conventional BLC operating in the same frequency of 6GHz.

Table 1. The design specifications of the suggested BLC.

Description	Notation	Dimension (mm)	Description	Notation	Dimension (mm)
Lengths of input arm (P_1) and Isolated arm (P_3)	L_I	9.27	Coupled arm (P4) length	L_c	10.02
All ports' width	W_I	1.53	Via radius	V_R	0.765
Horizontal arm (port) length	L_H	8.69	Substrates' thickness	H_1&H_2	0.8
Horizontal arm (port) Width	W_H	2.42	Substrates' Length	L_S	18
Output arm (P2) length	L_o	8.52	Substrates' Width	W_S	8.5

Preprints (www.preprints.org) | NOT PEER-REVIEWED | Posted: 18 December 2023 doi:10.20944/preprints202312.1281.v1

Horizontal arm (port) Width	W_H	2.42	Open-circuited stub length	L_{ST}	0.625
Open-circuited stub width	W_{ST}	0.375	Actual circuit area	$L_c \times W_c$	18×6.42

Step2: A periodically loaded slow wave structure shown in Figure 9(any reference to the slow wave structure or figure that you can show explicitly?? – I think this will be Figure 9) is adopted to design a compact $\lambda_g/4$ line with enhanced bandwidth to be accommodated the space limitation introduced due to the folding of the BLC halves and using a double layered Z-shaped meandering technique to realize compactness [18].

The idea behind a slow wave structure involves the incorporation of shunt capacitors at regular intervals along the length of the transmission line, as illustrated in Figure 9. This technique results in decreasing both the characteristic impedance and phase velocity, as also can be modelled from equations 7 and 8 below [18]:

$$Z_{o-Loaded} = \sqrt{\frac{L}{C + \frac{C_p}{d}}} \tag{7}$$

$$V_{p-Loaded} = \frac{1}{\sqrt{L(C + \frac{C_p}{d})}} \tag{8}$$

where, C_p represents the periodically added capacitor at a distance d along the transmission line. Z_{0_loaded} and Z_0 denote the characteristic impedance of the loaded and unloaded lines, respectively. On the other hand, reducing the phase velocity facilitates the achievement of an effectively longer electrical length by utilizing a physically shorter length. Additionally, to obtain a line with a specific characteristic impedance, the loading section (W_n) should possess a higher characteristics impedance, such that its characteristic impedance is decreased to the desired characteristic impedance, usually of 50Ω impedance, after loading.

The relation between the physical length l_p and the electric length l_e of the periodically loaded stub TL is given as [18]:

$$l_e = l_p \left(\frac{\omega_0}{V_{p-Loaded}} \right) \tag{9}$$

The added capacitance C_p, in terms of the known parameters of the loaded and unloaded TL, is given as [19]:

$$C_p = \frac{\phi}{N\omega_0} \left(\frac{Z_o^2 - Z_{o\_loaded}^2}{Z_o^2 Z_{o\_loaded}} \right) \tag{10}$$

where ω_0 is the angular frequency, and N is an integer that refers to the stub section's number.
On the other hand, open stubs with a length of multiples of a quarter wavelength were added in parallel to one pair of branch-line coupler sides, operating as a parallel stub transformer, as reported in [20]. Therefore, the characteristic impedance of the added stubs attenuates the maxima in return loss characteristics (S11) when the frequency deviates, which, in turn, broadens the bandwidth.
In the proposed configuration, shown in Figure 8, the slow wave structure is accomplished by inserting alternate slots around the conventional straight MSTL with respective length and width of 2.62 mm and 1.52 mm, which creates rectangular stubs around both sides of the line as shown in Figure 9c . To create rectangular stubs around the MSTL, slots were placed in an alternate configuration, resulting in stub dimensions of $W_{st} \times L_{st} = 0.234$ mm² on both sides of the line as depicted in Figure 9c. The addition of these slots transforms the 50Ω MSTL to a narrow MSTL with a width of W_n=0.271mm that provides a characteristic impedance of 105.9Ω, which compensates for the shunt

Preprints (www.preprints.org) | NOT PEER-REVIEWED | Posted: 18 December 2023 doi:10.20944/preprints202312.1281.v1

impedances of the periodic stubs and results in an overall characteristic impedance that is close to 50Ω.

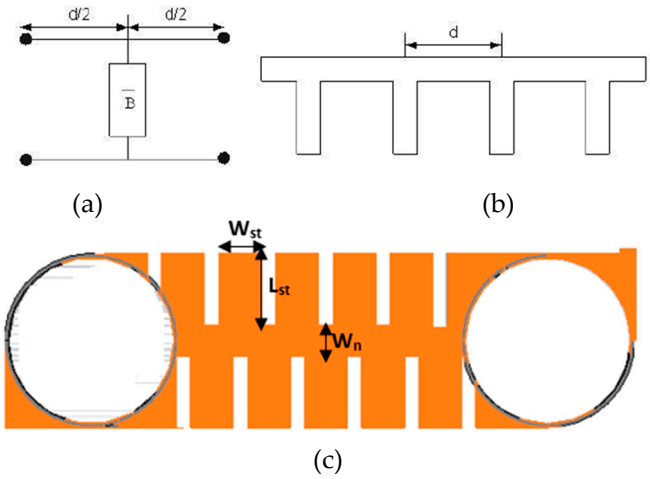

Figure 9. (a) A single periodic section circuit diagram of periodically loaded transmission line, (b) Schematic diagram of periodically loaded line with open stub used as loaded capacitance, and (c) The proposed slow wave structure.

4. Fabrication and Measurements

The proposed novel miniaturized BLC, shown in Figure 10, was fabricated on an FR4 substrate with a dielectric constant of 4.4 and a thickness of 0.8 mm, where a thin ground plane, of 70μm thickness, was inserted between the two FR4 substrates, forming a sandwich-like structure. Both substrates were truncated at their corners by a cross-sectional area of 2×5 mm each to expose the ground plane and enable the SMA connector to be easily connected, as illustrated in Figure 10b.

The fabricated novel BLC was measured using an HP 8720B Vector Network Analyzer (VNA), as shown in Figure 10c. The reflection coefficient, isolation coefficient between input ports 1 and 3, as well as the transmission and coupling coefficients were measured by connecting the relevant ports to the VNA, while the remaining ports were terminated by a 50Ω load to prevent additional mismatch and increase measurements' reliability, as illustrated in Figure10d.

As per the design specifications of the proposed BLC, the required phase difference between the output signals is 90°. This phase difference can be verified by measuring the phases of the transmission coefficients, S_{21} and S_{43}, and coupling coefficients, S_{41} and S_{23}, at the output ports 2 and 4. Once these measurements are carried out, the phase difference can be determined as:

$$\varphi = \begin{cases} \angle S_{21} - \angle S_{41} & \text{for input from port 1} \\ \angle S_{43} - \angle S_{23} & \text{for input from port 3} \end{cases} \quad (11)$$

(a) (b)

Preprints (www.preprints.org) | NOT PEER-REVIEWED | Posted: 18 December 2023 doi:10.20944/preprints202312.1281.v1

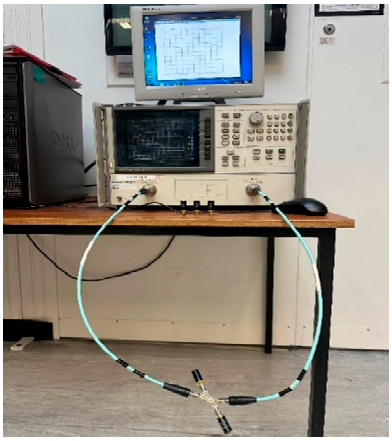

(c)

(d)

Figure 10. (a) BLC prototype, (b) BLC prototype with SMA connectors, (c) Measurement setup system, and (d) Termination of un-fed ports.

The performance of the proposed BLC is evaluated by observing the 4-port S-parameters magnitudes and phase difference as shown in Figure 11. The four principal scattering parameters considered in the analysis are: the reflection coefficient (RC) S_{11}, transmission coefficient (TC) S_{21}, isolation coefficient (IC) S_{31}, and coupling coefficient (CC) S_{41}, when port 1 is excited as the input port. On the other hand, when port 3 is excited, the required scattering parameters S_{13}, S_{23}, S_{33}, and S_{43} are considered. Ports 1 and 3 were chosen as they are located on opposite sides of the coupler and are designated as input ports. In addition, from Figure 11a it is evident that a good agreement is accomplished between the simulated and measured reflection coefficient. For example, the measured -10 dB S_{11} bandwidth extends from 4.6 GHz to 10GHz, which corresponds to a relative bandwidth 73.9% compared to a typical bandwidth of ~ 40% from an identical traditional branch line coupler. As a result, the proposed configuration offers a substantial bandwidth enhancement.

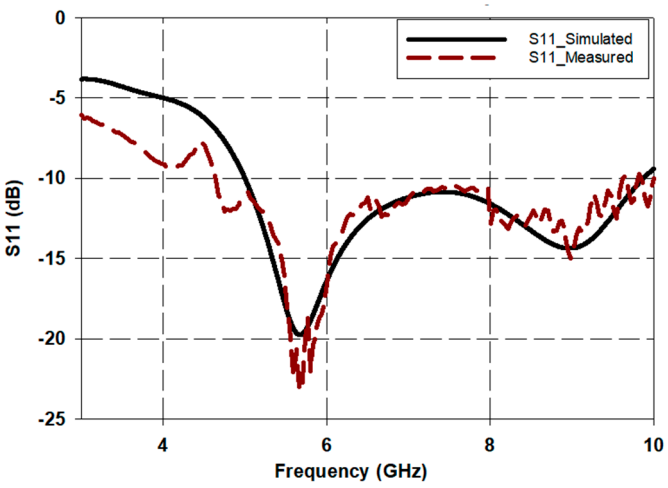

(a)

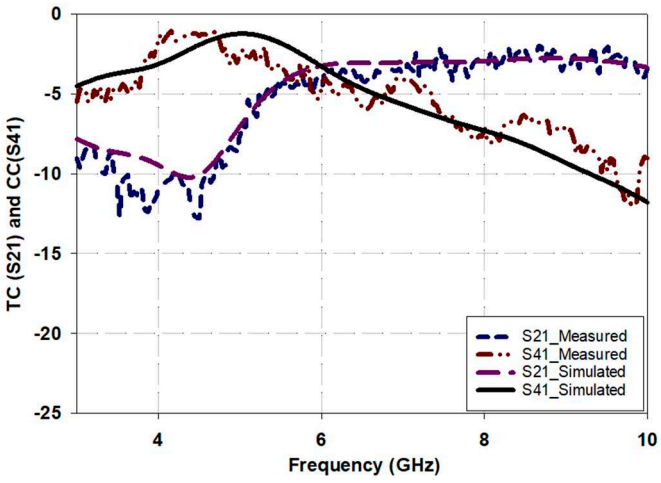

(b)

Preprints (www.preprints.org) | NOT PEER-REVIEWED | Posted: 18 December 2023 doi:10.20944/preprints202312.1281.v1

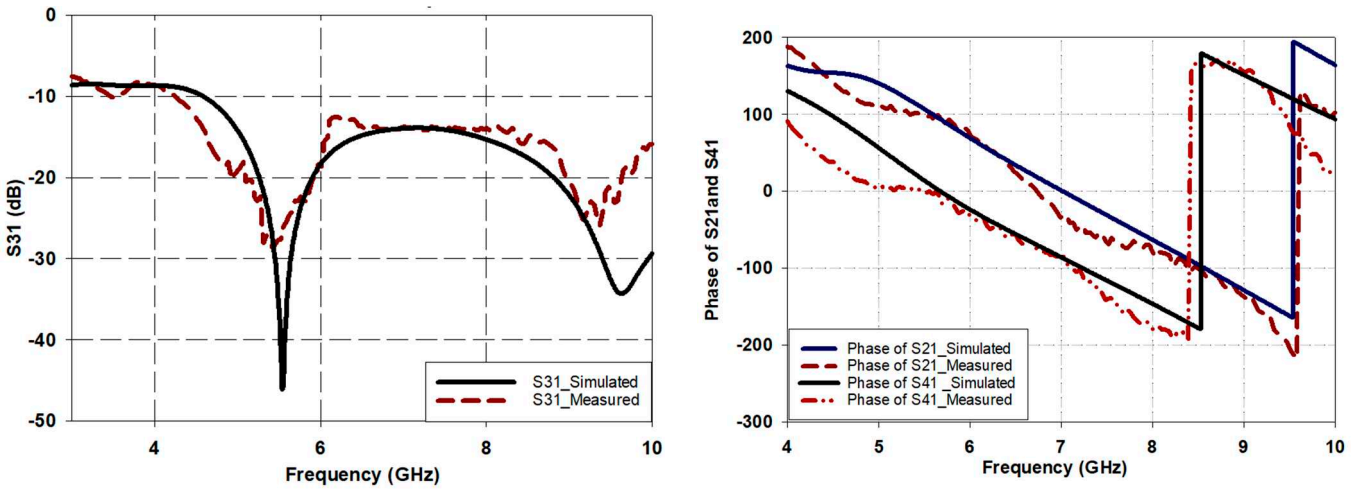

(c) (d)

Figure 11. 4-Port S-parameters for the proposed BLC when port 1 is excited, (a) S_{11}, (b) S_{21}, (c) S_{31}, (d) phase difference of the output power. .

The transmission and coupling coefficient, S_{21} and S_{41}, respectively, are presented in Figure11b with good agreement between measurements and simulations. From these results, it can be observed that both the transmission and coupling coefficients are -3.9 dB at the desired frequency of 6 GHz, which is close to the ideal value of -3 dB. Notably, S_{21} remains higher than -3.5 dB for the entire operating band ranging from 5.8 GHz to 10 GHz. However, the coupling coefficient S_{41} gradually degrades with increasing frequency, possibly due to vias and substrate losses since the input port and coupled ports are located on opposite sides of different substrates. Despite this degradation, the power delivered to port 4 remains greater than -7.5 dB up to a frequency of 8 GHz.

Furthermore, the isolation coefficient between the input ports, S_{31}, as shown in Figure 11c demonstrates a magnitude of less than -13 dB throughout the operating band, signifying a good isolation between input ports. This ensures that the proposed BLC meets the necessary design specifications for optimal performance.

Finally, Figure 11d presents the difference between the phases at the output ports 2 and 4 for input excitations from port 1. As the require a 90° phase difference between the output signals. At the design frequency of 6 GHz, the phase difference between output ports for input from port 1 is ($\angle S_{21}$-$\angle S_{41}$=90.50°), which satisfies the required phase difference for typical BLC design specifications. In addition, the phase difference error (PDE) is 0.5° for the deigned frequency of 6 GHz, which is marginal.

Figure 12 presents the proposed BLC performance when port 3 is excited. From Figure 12a it is evident that the -10 dB S_{33} bandwidth extends from 4.5GHz to 10GHz, which corresponds to a relative bandwidth of 75.8% compared to ~40% for the traditional branch line coupler based on the same design specifications and operating frequency of 6GHz. It should be noted that a marginal difference of 1.9% occurs between the reflection coefficients' bandwidth of S_{11} and S_{33}. The transmission coefficient, S_{23}, and the coupling coefficient, S_{43}, for port 3 excitations are illustrated in Figure 12b. At the target band, i.e at 6 GHz, the transmission, and the coupling coefficients of the proposed BLC design are -3.9 dB, which is close to the ideal value of -3 dB. Notably, the transmission coefficients S_{43} remain higher than -3.5 dB for the entire operating band ranging from 5.8 GHz to 10 GHz, and this behavior is consistent throughout this wide operating frequency range. However, the coupling coefficient S_{23} gradually degrades with increasing frequency, and this is due to using vias as well as losses inherited from the lossy FR4 substrates, as the input port and coupled ports are located on opposite sides of different substrates. Despite this degradation, the power delivered to port 4 remains greater than -7.5 dB up to a frequency of 8 GHz. In Figure 12c, the isolation coefficient between input ports, S_{13}, is depicted. It is evident that S_{13} remains less than –14 dB throughout the operating band. It can be concluded that the proposed miniaturized BLC has excellent performance in terms of scattering parameters (S-parameters) compared to a traditional BLC design. Additionally, based

Preprints (www.preprints.org) | NOT PEER-REVIEWED | Posted: 18 December 2023 doi:10.20944/preprints202312.1281.v1

on the obtained results, it can also be confirmed that the ports are reciprocal and have the same S-parameters characteristics for all ports. This consolidates the principle that the proposed miniaturized BLC can be used as a unit cell for constructing a Butler matrix, which in turn has the potential use in the development of phased array antenna systems.

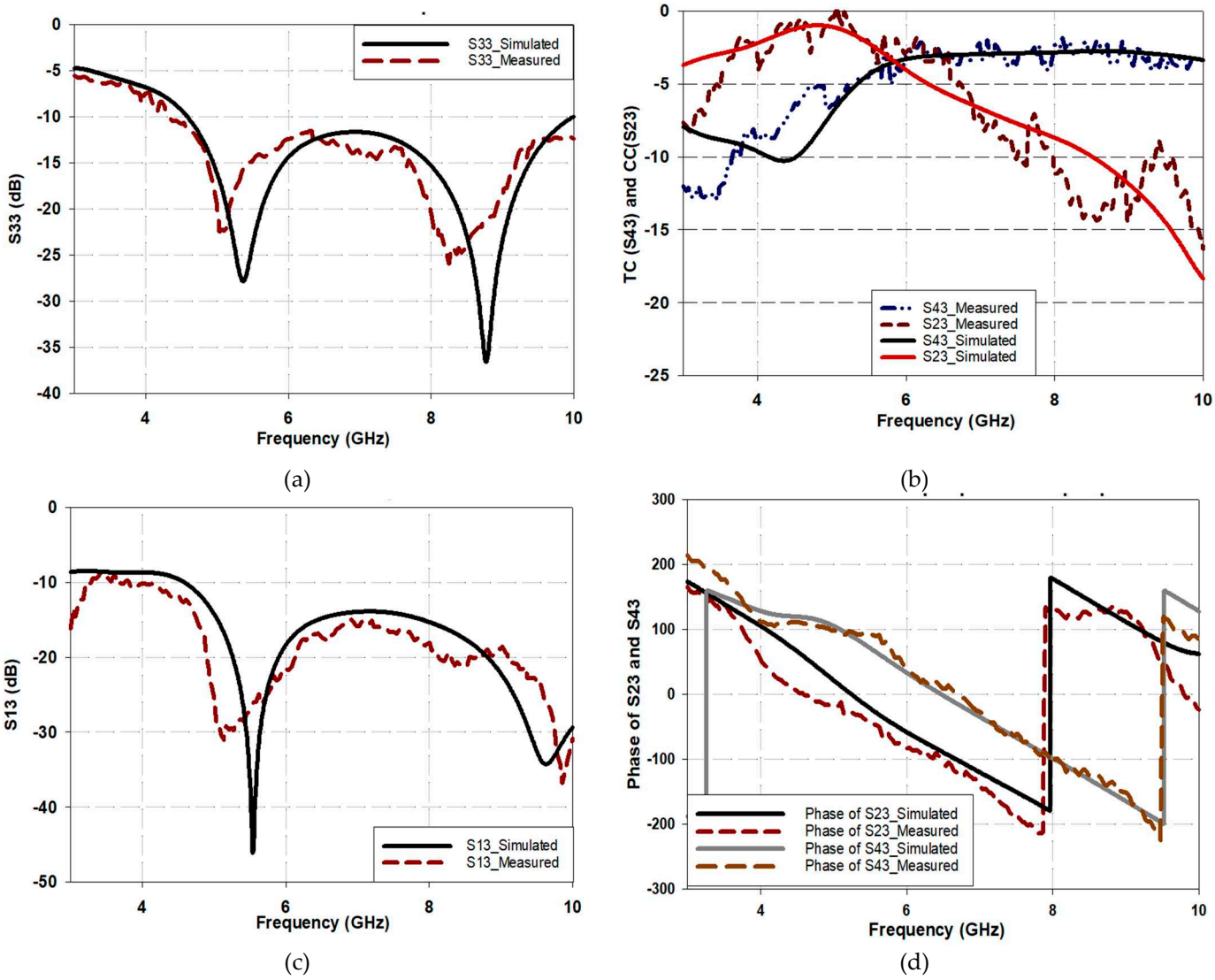

Figure 12. Performance of the proposed BLC when port 3 is excited, (a) S_{33}, (b) S_{43}, (c) S_{13}, (d) phase difference of the output power.

Figure 12d illustrates the phase difference between output ports 2 and 4 for input excitations from port 3. At the frequency of 6 GHz, the phase difference between output ports for input from port 3 ($\angle S_{43}$-$\angle S_{23}$=94.8°) which meets the requirements of a BLC coupler for good performance. However, a slight discrepancy between the simulated and measured phases is observed for input port 3. This difference may be attributed to fabrication tolerance and the lump solder for SMA feeders. Nevertheless, the phase difference error (PDE) at the design frequency of 6 GHz is 4.8° for the input port 3 excitation.

Table 2 provides a comparison between the performance of the proposed BLC and those of previously published BLC designs. Most of the designs presented in Table 2 were focused on either improving the bandwidth or reducing the size of the BLC. The proposed work, however, achieves both bandwidth enhancement and size reduction, which is crucial for the design of a 5G system. Furthermore, comparing with respect to the literature, the proposed miniaturized wide band BLC

 doi:10.20944/preprints202312.1281.v1

offer other advantages such as; design simplicity, easy to fabricate, smaller phase difference error, and equal power distribution among output port at design frequency 6GHz.

Table 2. Comparison of proposed BLC performance with respect to published designs available in the literature.

Ref.	Operating Frequency (GHz)	Relative Bandwidth (%)	Size (λ_g^2)	S_{11} @ 6GHz (dB)	S_{21} @ 6GHz (dB)	S_{41} @ 6GHz (dB)	S_{31} @ 6GHz (dB)	PDE error (Deg)
[4]	3.5	30.22	0.27 ×0.16	-27.47	-4.4	-3.1	-26.2	3.54
[5]	2.36	31.77	0.25 ×0.29	-25.5	-2.9	-3.2	-27.5	1
[7]	1.77	7.2	0.62 ×0.62	-35.9	-3.1	-3	-37.9	-
[8]	0.9	67.7	0.2 ×0.2	-19.89	-3.69	-3.67	-17.5	-
[9]	3	50.4	0.45×0.25	-21	-0.95	-10.5	-29	±10
[1]	3.5	40.2	0.55×0.65	-12	-3.19	-2.8	-15.2	-2
[11]	0.95	22.2	0.17×0.08	-30	2.3	-3.2	29	-
[12]	2.4	33.3	0.2×0.35	-20	12.5	-2.5	-20	±13
[13]	2	13 (S11<-20)	0.3×0.3	-30	-3.5	-3.5	-27	±5
This Work	6	75.8	0.3×0.74	-14	-3.17	-3.17	-18.9	0.5

5. Conclusion

A novel quasi-twisted miniaturized wideband branch line coupler has been introduced, which employs a Z-shaped meandered microstrip line with a slow wave structure on a double-layer substrate. The performance of the proposed design has been evaluated demonstrating agreement between the simulation and measurements and showing advantages over conventional microstrip branch line couplers in terms of size reduction and band improvement.

The novel quasi-twisted miniaturized wideband branch line coupler operates within the frequency band of 4.5 GHz to 10 GHz, offering a high relative bandwidth of up to 75.8% and reducing the size by 49.9% compared to conventional branch line couplers with a general bandwidth of 42.2%. A comparison between the proposed branch line coupler and the conventional design indicates that the former exhibits favorable scattering parameter specifications. Furthermore, the obtained results suggest that the ports of the branch line coupler demonstrate reciprocity, benefiting from consistent S-parameter characteristics across all ports. As a result, the proposed branch line coupler holds the potential to be integrated into a compact and wideband Butler matrix for future deployment in phased antenna array systems for potential use in 5G applications.

References

1. A. K. Vallappil, M. K. A. Rahim, B. A. Khawaja, and M. Aminu-Baba, "Metamaterial based compact branch-line coupler with enhanced bandwidth for use in 5G applications," *The Applied Computational Electromagnetics Society Journal (ACES)*, pp. 700-708, 2020.
2. J. Zhang, X. Ge, Q. Li, M. Guizani, and Y. Zhang, "5G millimeter-wave antenna array: Design and challenges," *IEEE Wireless communications*, vol. 24, no. 2, pp. 106-112, 2016.
3. S. Gomha, E.-S. M. El-Rabaie, A.-A. T. Shalaby, and A. S. Elkorany, "Design of new compact branch-line coupler using coupled line dual composite right/left-handed unit cells," *J. Optoelectron. Adv. Mater*, vol. 9, pp. 836-841, 2015.
4. A. A. Abdulbari, S. K. A. Rahim, M. Z. A. Abd Aziz, K. G. Tan, N. Noordin, and M. Nor, "New design of wideband microstrip branch line coupler using T-shape and open stub for 5G application," *International Journal of Electrical and Computer Engineering*, vol. 11, no. 2, p. 1346, 2021.
5. H. Alhalabi *et al.*, "Miniaturized branch-line coupler based on slow-wave microstrip lines," *International Journal of Microwave and Wireless Technologies*, vol. 10, no. 10, pp. 1103-1106, 2018.
6. W. L. Chen and G. M. Wang, "Design of novel miniaturized fractal-shaped branch-line couplers," *Microwave and optical technology letters*, vol. 50, no. 5, pp. 1198-1201, 2008.

7. S. Gomha, M. EL-Sayed, A. A. T. Shalaby, and S. Ahmed, "Miniaturization of Branch-line couplers using open stubs and stepped impedance unit cells with meandering transmission lines," *Circuits and systems: An international journal (CSIJ),* vol. 1, no. 3, pp. 13-26, 2014.
8. K. V. P. Kumar and A. J. Alazemi, "A flexible miniaturized wideband branch-line coupler using shunt open-stubs and meandering technique," *IEEE Access,* vol. 9, pp. 158241-158246, 2021.
9. M. Kumar, S. N. Islam, G. Sen, S. K. Parui, and S. Das, "Design of miniaturized 10 dB wideband branch line coupler using dual feed and T-shape transmission lines," *Radioengineering,* vol. 27, no. 1, pp. 207-213, 2018.
10. W. Nie, K.-D. Xu, M. Zhou, L.-B. Xie, and X.-L. Yang, "Compact narrow/wide band branch-line couplers with improved upper-stopband," *AEU-International Journal of Electronics and Communications,* vol. 98, pp. 45-50, 2019.
11. H. Siahkamari, M. Jahanbakhshi, H. N. Al-Anbagi, A. A. Abdulhameed, M. Pokorny, and R. Linhart, "Trapezoid-shaped resonators to design compact branch line coupler with harmonic suppression," *AEU-International Journal of Electronics and Communications,* vol. 144, p. 154032, 2022.
12. X.-Z. Wang, F.-C. Chen, and Q.-X. Chu, "A Compact Broadband 4 × 4 Butler Matrix With 360◦ Continuous Progressive Phase Shift," *IEEE Transactions on Microwave Theory and Techniques,* 2023.
13. H. Mextorf and W. Schernus, "A Novel Branch-Line Coupling Topology," *IEEE Transactions on Microwave Theory and Techniques,* 2023.
14. S. Roshani, S. I. Yahya, S. Roshani, and M. Rostami, "Design and fabrication of a compact branch-line coupler using resonators with wide harmonics suppression band," *Electronics,* vol. 11, no. 5, p. 793, 2022.
15. D. M. Pozar, *Microwave engineering*. John wiley & sons, 2011.
16. T. C. Edwards and M. B. Steer, *Foundations for microstrip circuit design*. John Wiley & Sons, 2016.
17. H. Tian, J. Gao, M. Su, Y. Wu, and Y. Liu, "A novel 3D two-ways folded microstrip line and its application in super-miniaturized microwave wireless components," *Journal of Electromagnetic Waves and Applications,* vol. 29, no. 3, pp. 364-374, 2015.
18. K. Rawat and F. Ghannouchi, "Design of reduced size power divider for lower RF band using periodically loaded slow wave structure," in *2009 IEEE MTT-S International Microwave Symposium Digest*, 2009, pp. 613-616: IEEE.
19. K. W. Eccleston and S. H. Ong, "Compact planar microstripline branch-line and rat-race couplers," *IEEE Transactions on microwave theory and techniques,* vol. 51, no. 10, pp. 2119-2125, 2003.
20. B. Mayer and R. Knochel, "Branchline-couplers with improved design flexibility and broad bandwidth," in *IEEE International Digest on Microwave Symposium*, 1990, pp. 391-394: IEEE.